

# Study of morphology and band gap energy of TiO<sub>2</sub>-carbon nanotube nanocomposite

F. Taleshi

Received: 1 December 2014 / Accepted: 6 February 2015 / Published online: 11 February 2015  
© Springer Science+Business Media New York 2015

**Abstract** The present work aims to study the synthesis, morphology and optical properties of TiO<sub>2</sub>/CNT nanocomposite. TiO<sub>2</sub>/CNT nanocomposite powder were synthesized by sol–gel method using TiCl<sub>4</sub> as a precursor in ethanol solution containing CNTs as a support. The prepared samples were characterized by scanning electron microscopy, powder X-ray diffraction, transmission electron microscopy and Fourier transform infrared spectroscopic techniques. The results show that TiO<sub>2</sub> nanoparticles covered a homogenous layer on the surface of purified CNTs. Moreover, applying CNTs as a support can significantly change the morphology and band gap energy of TiO<sub>2</sub> nanoparticles.

## 1 Introduction

In recent years, the synthesis and characterization of new nanostructure have received much attention due to their significant potential application [1–3]. On the other hand, the specific properties of nanoparticles are closely related to their size and distribution. Regular morphology, highly distributed nanoparticles with small size and narrow size distribution are ideal for various applications, such as high electrocatalyst activity [3, 4], optical properties [5–7] and antibacterial activity [8], owing to large surface-to-volume ratio.

Fabricating CNT-supported nanomaterial is thereby desirable since it combines both the advantages of CNTs

and nanomaterial, which may be useful in expanding the applications [3, 9, 10].

In recent years, TiO<sub>2</sub> nanoparticles have received much attention due to their excellent biocompatibility, optical properties, unique electronic and catalytic properties [11–13]. The properties of the titanium oxide is highly dependent on their nonstructural characteristic, including phase and crystal size, morphology, aspect ratio and even distribution density [4, 12, 14–17]. Due to the chemically ‘inert’ characteristic and the highly hydrophobic nature of CNTs surface, it is difficult to make attachment with metal precursors [1–3, 9, 10, 18]. Then, the surface modification is required so as to establish efficient tube–nanoparticles interactions are established. The extensive dispersion of various functional groups such as hydroxyl, carboxyl and carbonyl on CNTs surface could provide active sites with metal ions to attach [2, 9, 10, 18]. Different from the previously reported methods, TiO<sub>2</sub>/CNT composite is produced by modifying CNTs to achieve high dispersion, suitable morphology and better size distribution of TiO<sub>2</sub> nanoparticles [5, 9–12, 19]. Therefore, it is desirable to develop a simple and effective synthesis route that provides homogeneously dispersed TiO<sub>2</sub> nanoparticles while maintaining some degree of control over particle size and size distribution of CNTs. Modifying CNTs surface with desired functional groups by chemical treatments is a common strategy to get well-dispersed TiO<sub>2</sub> nanoparticles on CNTs [9–12, 19]. Moreover, TiO<sub>2</sub> nanoparticles prepared in ethanol solution by sol–gel technique, maintained their small particle size and narrow size distribution deposited on the surface of CNTs [14, 20]. Although these strategies are effective, the controllability has not been fully known.

In the present study, the main purpose is to demonstrate a simple and general procedure for the decoration of CNTs with TiO<sub>2</sub> nanoparticles. More importantly, the content of

---

F. Taleshi (✉)  
Department of Applied Science, Qaemshahr Branch,  
Islamic Azad University, PO Box 163, Qaemshahr, Iran  
e-mail: far.taleshi@gmail.com

TiO<sub>2</sub> supported on CNTs can be appropriately controlled by simply tuning the relative ratio of TiO<sub>2</sub> to CNTs. We have measured the optical absorption and band gap energy of TiO<sub>2</sub> nanoparticles with rutile and anatase structures by UV–Vis spectroscopy. The results indicate that application of CNTs as a support can decrease the value of band gap energy, censurability.

## 2 Experimental

CNTs were produced by chemical vapor deposition method using acetylene cracking over Co<sub>3</sub>O<sub>4</sub>/MgO catalyst-support. The process of synthesis had been described earlier [21]. The raw product contains impurities such as the support, catalyst particles, and a few amorphous carbons. The as-grown CNTs were purified using a two-step purification procedure involving thermal treatment at 490 °C for 2 h under air flow condition and then were sonicated for 30 min in a mixture of concentrated nitric acid/sulfuric acid (5 M and 1:1 by volume) and stirred for 4 h. This suspension was filtered and then washed several times with distilled water to acid-free, and finally dried at 120 °C for 2 h.

TiO<sub>2</sub>/CNTs nanocomposite was prepared using sol–gel technique. For the decoration of CNTs, in a typical synthesis, 0.2 g of functionalized CNTs were dispersed into ethanol solution by ultrasonication for 10 min. Afterward, a desired amount of titanium tetrachloride (99.5 %, Merck) was slowly added dropwise into ethanol solution containing functionalized CNTs under stirring. The size of TiO<sub>2</sub> nanoparticles were controlled by the ratio of TiO<sub>2</sub> to CNTs. In order to achieve different weight ratio of TiO<sub>2</sub> to CNTs (1:0, 1:1, 1:2, 1:4, 1:8 and 1:12) in nanocomposites, we selected the desired value of TiCl<sub>4</sub> in solution. For each synthesis, the ratio of TiCl<sub>4</sub> to ethanol was 1:10.

The solution was stirred for 24 h under atmospheric presser and temperature of 24 °C. Each sol–gel solution was vaporized at 80 °C in environmental conditions, until a dry-gel was obtained. The dry-gel was dried overnight in an oven at 120 °C. The TiO<sub>2</sub> powders were grounded using mortar and pestle. The as-prepared samples were calcinated at 400 °C in a tubular electrical furnace under argon gas atmosphere (at ramping rate of 10 °C/min) for 2 h.

## 3 Results and discussion

### 3.1 Characterizations of synthesized materials

The crystal structure of samples was investigated by X-ray diffraction [GBC, Cu (K<sub>α</sub>) Spectra, λ = 1.54 Å] in 2θ ranging from 10° to 90°. A scanning electron microscope

(SEM, Philips, 15 kV, 60 kx), transmission electron microscopy (TEM, Philips, CM10, 100 kV) were used to check the morphology of nanocomposites. FT-IR apparatus (Shimadzu—8400 s) was used to identify the functional groups on the surface of CNTs. UV–Vis spectra of TiO<sub>2</sub> nanoparticles were recorded by using of a spectrometer (GBC, Cintera 20). In addition, the sizes of TiO<sub>2</sub> nanoparticles were determined by Debby–Scherrer equation.

### 3.2 Structural and morphology analysis

In order to study the morphology of TiO<sub>2</sub>/CNT nanocomposites, SEM images prepared from all samples (Fig. 1). As Fig. 1a (1:0 ratio), due to surface activity, TiO<sub>2</sub> nanoparticles are seen as dense aggregates and make large particles. It is evident that the aggregated particles have irregular shape. This aggregation is not appropriate for physical and chemical applications and can decrease their unique properties. As SEM images (Fig. 1b–f), by using CNTs as a support, they prevented aggregation of TiO<sub>2</sub> nanoparticles. It can be observed that for lower ratio of CNTs (1:1 ratio, Fig. 1b), there is a nonuniform distribution of TiO<sub>2</sub> particles with irregular shapes. However, by increasing density of CNTs, the images clearly showed high homogeneity and good morphology of the particles which was strongly dependent on the ratio of TiO<sub>2</sub> to CNTs. At large ratio of CNTs to TiO<sub>2</sub> (Fig. 1f), the surface of purified CNTs is covered completely with TiO<sub>2</sub> nanoparticles and there is not any aggregated TiO<sub>2</sub> nanoparticles between interface of CNTs. The well-distributed nanoparticles deposited on surface of the carbon nanotubes demonstrate that the CNTs pretreatment processing was effective, which resulted in many active sites on the carbon nanotubes.

Figure (2) shows TEM images prepared from purified and decorated CNTs. Figure (2a) shows the morphological structure of CNTs where the crystalline tubular structure of nanotubes are observed. It is observed that the nanotubes have clear inner and outer surfaces. Figure (2b) displays typical TEM images of typical CNTs decorated with TiO<sub>2</sub> nanoparticles (with 1:1 ratios of TiO<sub>2</sub> to CNTs). It presents the morphology and the size distribution of TiO<sub>2</sub> nanoparticles on the sidewalls of the carbon nanotubes (dark spots) and the inner cavity of the tube still clear. It can be seen that the average size of TiO<sub>2</sub> nanoparticles is about 8.2 nm.

The Structure of TiO<sub>2</sub> powder and TiO<sub>2</sub>/CNTs nanocomposite samples have been investigated by XRD patterns. Figure 3 shows that the XRD patterns of the both TiO<sub>2</sub> powder and TiO<sub>2</sub>/CNT nanocomposite samples were calcinated at 400 °C.

The main diffraction peaks of the TiO<sub>2</sub> nanoparticles confirmed the good crystallite, which is well consistent

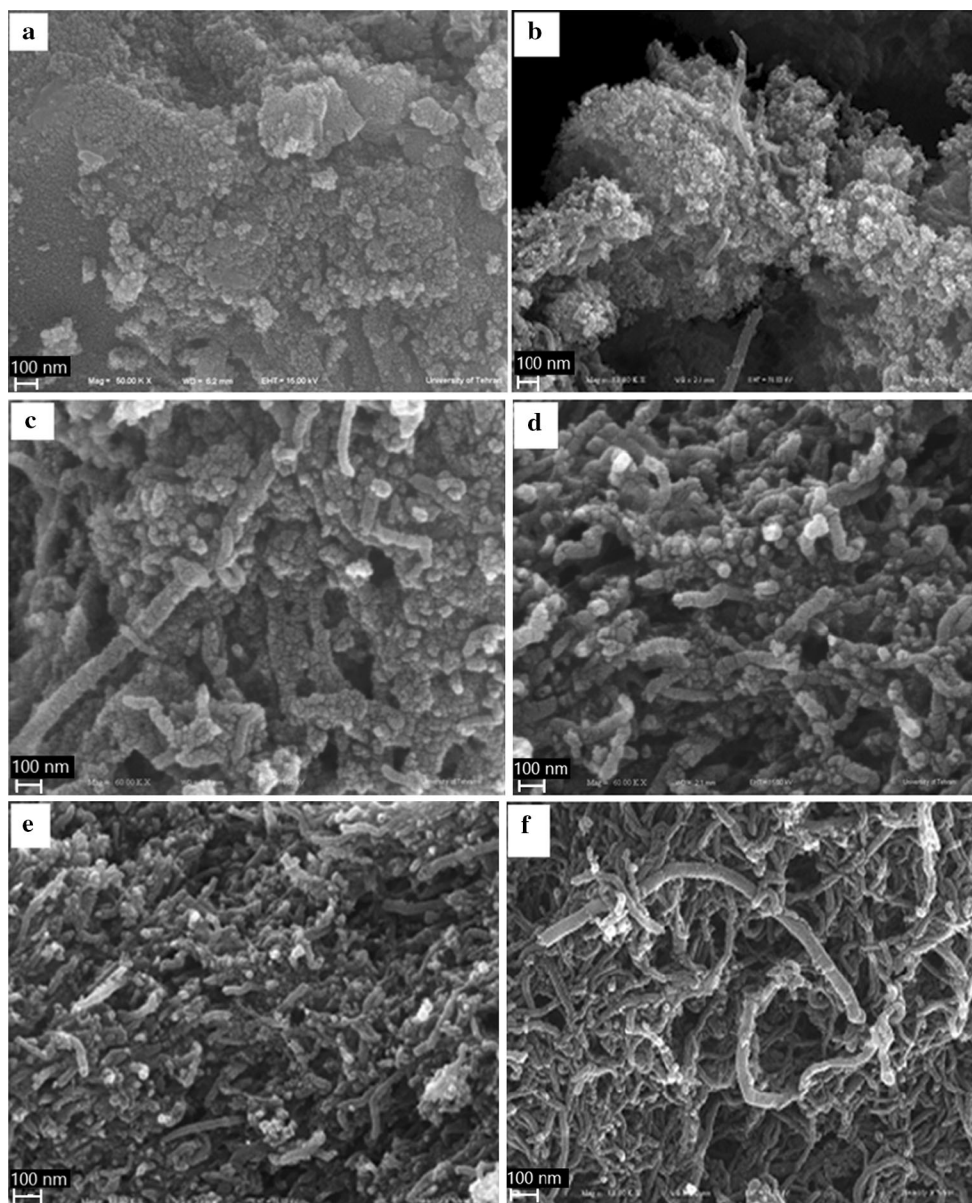


**Fig. 1** SEM images of TiO<sub>2</sub>/CNT samples calcinated at 400 °C for 2 h, **a** 1–0, **b** 1–1, **c** 1–2, **d** 1–4, **e** 1–8 and **f** 1–12 ratios. (The magnification of images is 60 kx)

with the results of other studies [14, 20]. In X-ray diffraction (XRD) patterns of TiO<sub>2</sub> and TiO<sub>2</sub>/CNTs the diffraction peak at  $2\theta$  of 25.4°, 37.9°, 48.1°, 54.8, 55.3°, 62.9°, 69.3°, 70.5°, 75.2°, 75.6° and 82.5°, which are attributed to anatase TiO<sub>2</sub> [20, 21]. There were also no any corresponding peaks to confirm the crystallization of rotail at this temperature for TiO<sub>2</sub> nanoparticles in all TiO<sub>2</sub>/CNT nanocomposites. Nevertheless, in XRD patterns of TiO<sub>2</sub>/CNT nanoparticles, the additional peak could be well seen at 26.06, which is corresponding to graphite [22]. Moreover, for all samples, observation of spectrum revealed that with the increasing the ratio of CNTs in nanocomposites,

the intensity of the TiO<sub>2</sub> peaks decreased significantly. The average crystallite size ( $D$ ) was calculated from maximum peak according to Debby–Scherrer’s formula [23]:

$$D = 0.9\lambda / (\beta \cos\theta) \quad (1)$$

where  $\lambda$  is the wavelength of the X-ray radiation (0.1541 nm),  $\theta$  is the Bragg’s angle in degree and  $\beta$  is the full width at half maximum (FWHM) of the peak in radian.

The XRD confirms that the highest intensity peaks were at  $2\theta = 26^\circ$ , which

corresponds to the reflection plane (311) and the average particle size was found to be 14.3, 8.6, 6.2, 4.7, 3.4, 2.1 nm

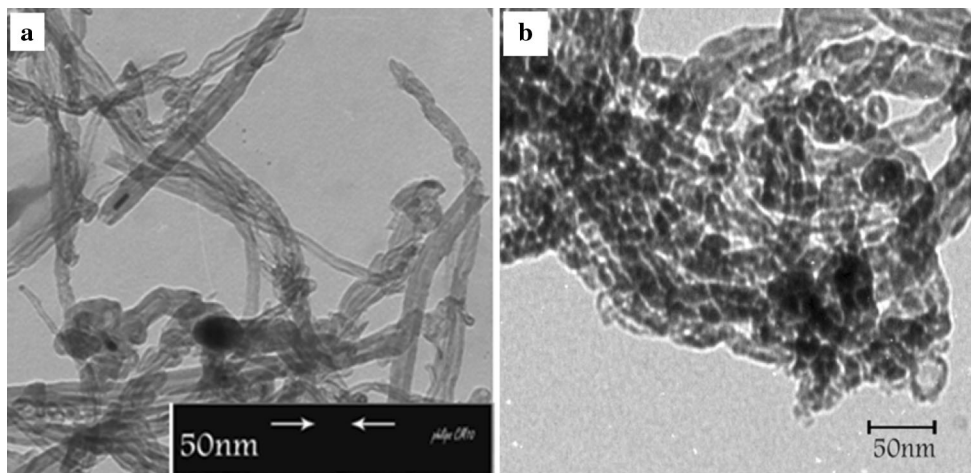


**Fig. 2** TEM images of purified CNTs (a) and TiO<sub>2</sub>/CNT nanocomposites in ratios of 1:1 (b), calcinated at 400 °C for 2 h

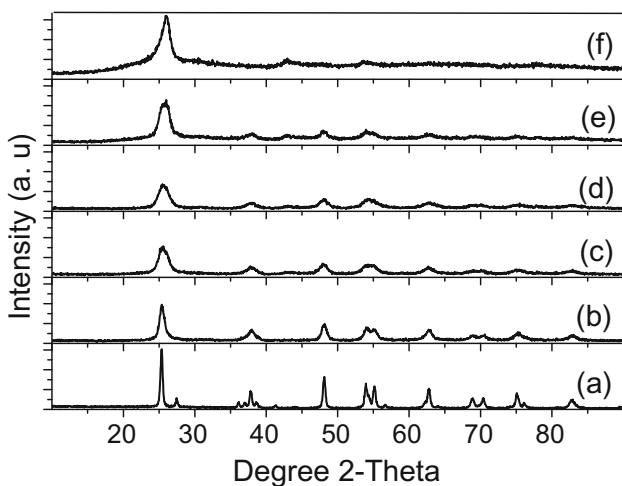


**Fig. 3** XRD pattern of TiO<sub>2</sub>/CNT samples calcinated at 400 °C for 2 h, a 1–0, b 1–1, c 1–2, d 1–4, e 1–8 and f 1–12 ratios

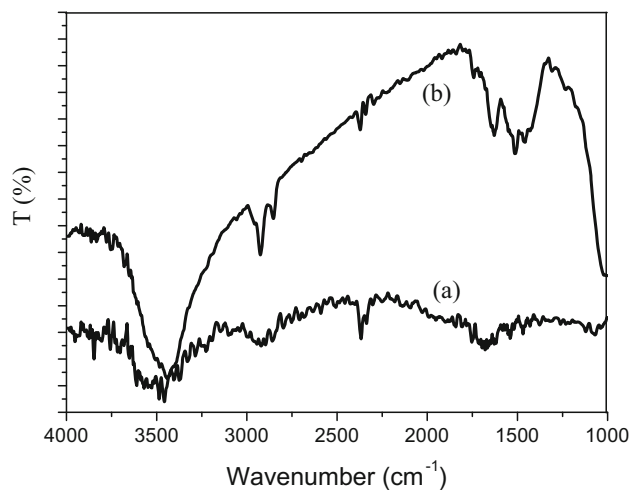


**Fig. 4** FT-IR spectra of pristine a and purified CNTs b

for 1:0, 1:1, 1:2, 1:4, 1:8 and 1:12 ratio, respectively. Accordingly, the particle sizes decreased with the increasing of the ratio of CNTs in nanocomposites ranging from 1:0 to 1:12, respectively.

The FTIR spectra of “as-prepared” and oxidized CNTs are compared in Fig. 4. The FT-IR spectroscopy study of oxidized CNTs confirms the defective sites at the surface of CNTs, and the presence of function groups O–C=O (1210/cm), C–O–O (1415/cm), C–O (1475/cm), and C=O (1,025 and 1720/cm) which leads to the hydrophilic nature of CNTs [18]. These functional groups may also act as stimulant in the formation of the composites, and enhance the interfacial bonding of TiO<sub>2</sub> nanoparticles with carbon nanotubes.

As a result, it is speculated that the TiO<sub>2</sub>/CNTs nanocomposite powder form the redox reaction between Ti

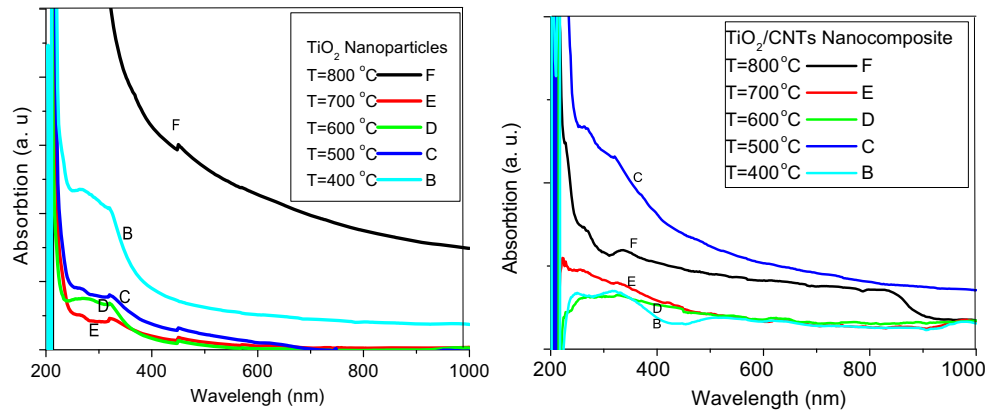
ions with functional groups on the surface of CNTs under sol–gel conditions. Then the bonding C–O–Ti or O=C–O–Ti might be formed between two materials and TiO<sub>2</sub>–CNTs composites were formed naturally through some physico-chemical bonding [18]. Consequently, Ti ions nucleated heterogeneously via sol–gel method because CNTs have prevented TiO<sub>2</sub> from growing into aggregated nanoparticles.

The optical properties of the synthesized TiO<sub>2</sub> nanoparticles and TiO<sub>2</sub>/CNTs nanocomposite were characterized by the UV–Vis spectroscopy (Fig. 5). The optical band gap of TiO<sub>2</sub> nanoparticles was determined from the absorption spectra by using Tauc equation [24]. The absorption coefficient,  $\alpha$  is related to the optical band gap energy ( $E_g$ ) by the relation:

$$(\alpha h\nu)^{1/n} = B(h\nu - E_g) \tag{2}$$



**Fig. 5** Optical absorption spectrum of TiO<sub>2</sub> nanoparticles and TiO<sub>2</sub>/CNTs nanocomposite (with 1:1 weight ratio of TiO<sub>2</sub> to CNTs) at different calcination temperatures



where  $h$  is the Plank's constant,  $\nu$  is the photon frequency of the radiation and  $B$  is the parameter of absorption edge width. The exponent  $n$  could be determined by the type of electronic transitions causing the optical absorption and it has taken the values of  $1/2$  and  $2$  for direct-allowed and indirect-allowed transition, respectively.

In the present case, the optical band gap for the absorption peak can be obtained by extrapolating the linear portion of the  $(\alpha h\nu)^2 - h\nu$  curve and the type of electronic transitions indirect-allowed transition (Fig. 6). The value of band gap energy ( $E_g$ ) of TiO<sub>2</sub> nanoparticles and TiO<sub>2</sub>/CNT nanocomposites are piloted as a function of different calcination temperatures (Fig. 7). As Fig. (7), the band gap energy of TiO<sub>2</sub> nanoparticles decrease by using CNTs as support, considerably. It is clearly that its value is alternated by increasing calcination temperature. As these experimental results, they show that the CNTs and different

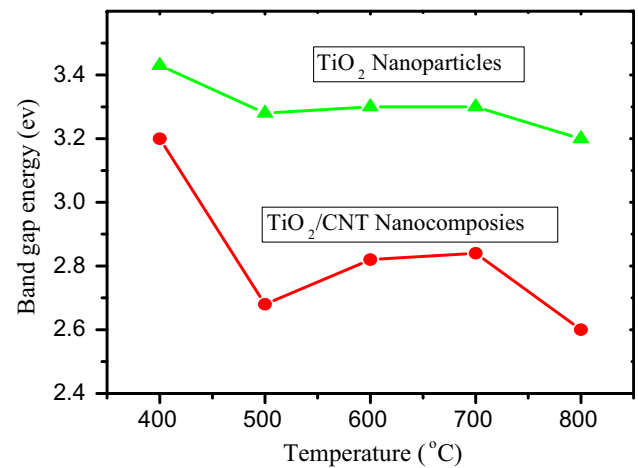


**Fig. 7** Diagram of band gap energy of TiO<sub>2</sub> nanoparticles and TiO<sub>2</sub>/CNT nanocomposites, (with 1:1 weight ratio of TiO<sub>2</sub> to CNTs) in terms of different calcination temperatures

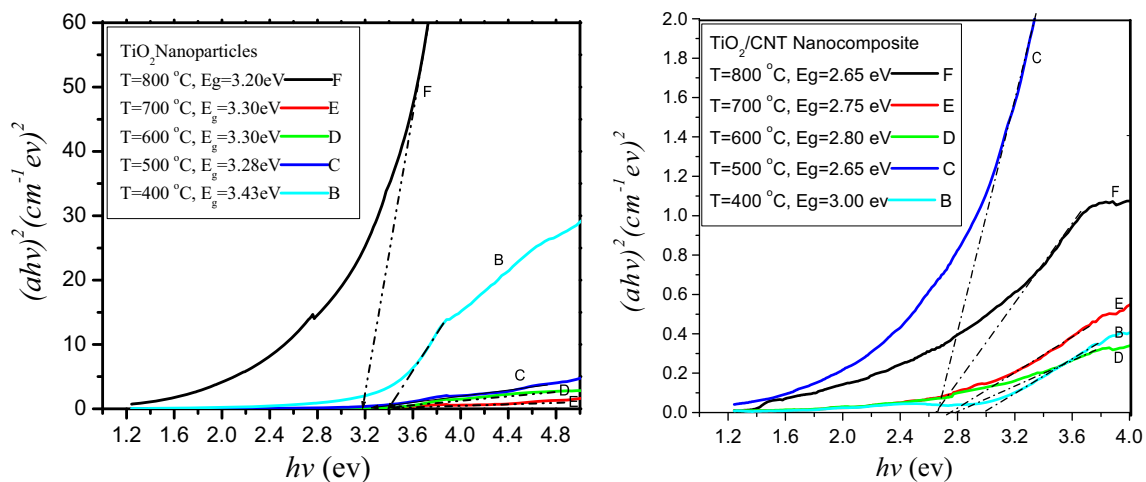


**Fig. 6** Extrapolating the linear portion of the  $(\alpha h\nu)^2 - h\nu$  curve for TiO<sub>2</sub> nanoparticles and TiO<sub>2</sub>/CNTs nanocomposite powders (with 1:1 weight ratio of TiO<sub>2</sub> to CNTs) at different calcination temperatures

calcination temperature can influence the band gap energies of the TiO<sub>2</sub> nanoparticles. By application of CNTs as a support of TiO<sub>2</sub> nanoparticles, this effect is probably due to increase in chemical defects or vacancies present in the intergranular regions and also chemical interaction between CNTs and TiO<sub>2</sub> nanoparticles, generating a new energy level to reduce the band gap energy [21, 25]. The TiO<sub>2</sub>/CNT nanocomposite with lower band gap energy are optically active and have been extensively used in the field of photo-oxidation catalysis for environmental cleanup and solar cell.

#### 4 Conclusions

The TiO<sub>2</sub> nanoparticles and TiO<sub>2</sub>/CNT nanocomposites have been successfully synthesized by sol-gel technique and their structural and morphology were studied. High efficiency of proposed method was confirmed as well as the possibility of the coating of TiO<sub>2</sub> nanoparticles over CNTs, without aggregation of these particles. The size of TiO<sub>2</sub> nanoparticles and morphology of powder are varied by changing the weight percent of carbon nanotubes in solution. The results show that application of CNTs as a support was decreased the band gap of TiO<sub>2</sub> nanoparticles.

#### References

1. X. Wang, Z. Zhao, J. Qu, Z. Wang, J. Qiu, J. Phys. Chem. Sol **71**, 673 (2010)
2. E.T. Thostenson, Z. Ren, T.W. Chou, Compos. Sci. Tech. **61**, 1899 (2001)
3. F. Gholami-Orimi et al., J. Anal. Methods Chem. (2001). doi:10.1155/2012/902184
4. S. Palmas et al., Int. J. Hydrog. Energ. **35**, 6561 (2011)
5. W.C. Oh, J. Korean Ceram. Soci. **46**, 234 (2009)
6. V. Etacheri, M.K. Seery, S.J. Hinder, S.C. Pillai, Adv. Funct. Mater. **21**, 3744 (2011)
7. A. Ramadoss, K. Krishnamoorthy, S.J. Kim, Mater. Let. **75**, 215 (2012)
8. E. Weir, A. Lawlor, A. Whelan, F. Regan, Analyst **133**, 835 (2008)
9. M.L. Chen, F.J. Zhang, W.C. Oh, New Carbon Mat. **24**, 159 (2009)
10. N. Bouazza et al., Appl. Catal. B Environ. **92**, 377 (2009)
11. S. Sarmah, A. Kumar, Indian J. Phys. **85**, 713 (2011)
12. H. Yu et al., J photochem photobiol A Chem. **200**, 301 (2008)
13. S. Yuen et al., Compos Part A **39**, 119 (2008)
14. H. Milani, Moghaddam and S Nasirian. S. Afr. J. Sci. **107**, 1 (2011)
15. P. Vincent et al., J. Non-Cryst. Sol. **311**, 130 (2002)
16. H.Y. Chuang, D.H. Chen, Int. J. Hydrog. Energ. **36**, 9487 (2011)
17. H. Omidvar, F.K. Mirzaei, M.H. Rahimi, Z. Sadeghian, New Carbon Mater. **27**, 401 (2012)
18. L. Chen, B.L. Zhang, M.Z. Qu, Z.L. Yu, Powd. Technol. **154**, 70 (2005)
19. A. Jitianu et al., Carbon **42**, 1147 (2004)
20. F. Taleshi, A. Pahlavan, J. Mater. Sci. Mater. Electron. **25**, 2450 (2014)
21. H. Milani Moghaddam, Nanosci. Methods **1**, 201 (2012)
22. F. Taleshi, A.A. Hosseini, Indian J. Phys. **87**, 425 (2013)
23. K. Venkateswarlu, A. Chandra Bose, N. Rameshbabu, Phys. B **405**, 4256 (2010)
24. J. Tauc, *Amorphous and Liquid Semiconductors* (Plenum Press, New York, 1974)
25. L. Sohrabi, F. Taleshi, R. Sohrabi, J. Mater. Sci. Mater. Electron. **25**, 4110 (2014)